Product directivity models for parametric loudspeakers

Chuang Shi

Email: shic0002@e.ntu.edu.sg

Tel: (65)67906901

Fax: (65)67933318

Digital Signal Processing Laboratory, School of Electrical and Electronic Engineering, Nanyang Technological University, Singapore

Address: S2-B4a-03, 50 Nanyang Avenue, Singapore 639798

Woon-Seng Gan

Email: ewsgan@ntu.edu.sg

Tel: (65)67904538

Fax: (65)67933318

Digital Signal Processing Laboratory, School of Electrical and Electronic Engineering, Nanyang Technological University, Singapore

Address: S2-B4a-03, 50 Nanyang Avenue, Singapore 639798

ABSTRACT

In a recent work, the beamsteering characteristics of parametric loudspeaker were validated in experiment. It was shown that based on the product directivity model, the locations and amplitudes of the mainlobe and grating lobes could be predicted within acceptable errors. However, the measured amplitudes of sidelobes have not been able to match with the theoretical results accurately. In this paper, the original theories behind the product directivity model are revisited, and three modified product directivity models are proposed: (i) the advanced product directivity model, (ii) the exponential product directivity model, and (iii) the combined product directivity model. The proposed product directivity models take the radii of equivalent Gaussian sources into account and obtain better predictions of sidelobes for the difference frequency waves. From the comparison between measurement results and numerical solutions, all the proposed models outperform the original product directivity model in term of selected sidelobe prediction by about 10 dB.

PACS numbers: 43.25.Lj, 43.60.Fg, 43.38.Fx

I. INTRODUCTION

The parametric loudspeaker has been demonstrated to be one of the most effective ways to generate a low frequency directional sound field. The discovery of the parametric array effect and its theoretical explanation can be traced back to 1963 when Westervelt[1] published his observation and equation on the generation of low-frequency wave (also known as the difference frequency wave), through the interaction of high-frequency waves (also known as the primary frequency waves). Subsequently, Bennett and Blackstock[2] brought the parametric acoustic array experiment from underwater to air. They verified experimentally that parametric array effect can also be generated in air, creating highly directional sound beam. In 1965, Berktay[3] analyzed the propagation effect of collimated primary plane waves along their propagating axes, and simplified the Westervelt's equation for a far-field solution. Till now, the Berktay's far-field solution is still widely used to evaluate the performance of parametric loudspeakers and provides important guidelines in designing preprocessing approaches to reduce harmonic distortions[4]. In 1969, Zabolotskaya and Khokhlov[5] developed a nonlinear parabolic wave equation for non-dissipative fluids, which describes the combined effects of diffraction and nonlinearity. Darvennes and Hamilton[6-7] investigated the scattering of sound by sound from Gaussian beams that intersect at moderate angles. A closed-form equation was derived and validated throughout the entire paraxial field. One observation derived from the closed-form equation is that the far-field directivity of the difference frequency wave is governed by the product of the primary beam directivities. This is commonly known as the product directivity (PD) model and used as the fundamental principle in many later works on beamsteering of parametric loudspeakers[8-11].

Based on the PD model, one of the earliest attempts on digital beamsteering approach for the parametric loudspeaker was carried out by Tan[8]. Each ultrasonic transducer in the parametric

loudspeaker was treated as one bifrequency Gaussian source, and thus, a constant-beamwidth beamformer was worked out for the difference frequency wave through simulation. Later, Olszewski[9] suggested that several guidelines known to conventional phase array theory could not be realized for parametric loudspeakers. Therefore, a hybrid system combining a digital phased array technique with mechanical tilting louvers was proposed. However, mechanical structure in the hybrid system is bulky in size, and cannot be easily scaled down. Furthermore, reflection caused by neighboring louvers leads to another problem of this hybrid system that degrades its ability to control the directivity of the sound beam accurately. Subsequently, Gan[10] studied the digital implementation of beamsteering algorithms for parametric loudspeakers. By applying separate delays to different primary signals, limitation of the steering angles caused by the sampling rate is circumvented, and the increase in computation can be readily handled by a baseband digital processor. More recently, Lee[11] proposed a beamsteerer with complex weights in place of time delays, which result in versatile transmitting beampatterns.

One application of steerable parametric loudspeakers that was implemented by Tanaka[12-13] is an active noise control system with a steerable beam control. In this system, a compact transducer array was fabricated with reduced spacing to suppress grating lobes in order to obtain a controllable directivity. However, in another recent development, the authors[14] have also verified the beamsteering capabilities of the parametric loudspeaker of two different transducer array configurations. These array configurations are achieved by grouping transducers into several channels in different grouping array and applying delay-and-sum approach to control the directivity of primary frequency waves. In addition, partial or full grating lobe eliminations were observed at the difference frequency generated from various primary frequency waves. But it is noted that there are some discrepancies between the measured directivities and the theoretical

beampatterns of the primary frequency waves. The mismatch problem becomes more evident when the measured directivities of the difference frequency waves are compared with the theoretical beampatterns derived from the PD model.

In this paper, we approximate the directivity characteristics of a linear ultrasonic transducer array by using an equivalent circular Gaussian source array, which satisfies the prerequisites of applying the PD model. Furthermore, we revisit the original theories behind the PD model and propose three modified product directivity models, namely, (i) the advanced product directivity model, (ii) the exponential product directivity model, and (iii) the combined product directivity model. The proposed product directivity models take the radii of equivalent Gaussian sources into account and can result in a better prediction of sidelobes for the difference frequency waves.

This paper is organized as follows. The theories and equations behind the PD model are examined and three proposed product directivity models are derived in Section II. In Section III, directivities at both the primary frequencies and the difference frequencies measured in experiments are used to compare with the numerical solutions to the proposed product directivity models and the PD model. Section IV summarizes the key findings in this paper.

II. THOERY

The nonlinear effect produced by sound beams whose axes intersect at nonzero angles is referred as scattering sound by sound[7]. The nonlinear interaction region is formed by the intersection of two non-collinear primary beams. When Gaussian sources are used to model the primary sound beams, a closed-form solution to the second-order wave equation can be derived from quasilinear approximation. A solution for the far-field directivity of the difference frequency wave is given by the product of the primary beam directivities regardless of whether primary sources are displaced and steered.[6] This solution, commonly known as the PD model,

has been used to design and predict the directivities of the parametric loudspeaker. However, the measured beampatterns of the difference frequency wave usually do not match the theoretical beampatterns perfectly. To solve this practical problem, we revisit the PD model, and propose three modifications to the PD model that are more applicable to predict the steerable beampatterns of the parametric loudspeakers.

(a) Gaussian source

In acoustics, Gaussian sources are acoustic sources with Gaussian amplitude shading. The advantage of considering Gaussian sources is its closed-form solution for second-harmonic pressure that can be derived from the quasilinear approximation.[7] The source function q_g of Gaussian sources is defined as

$$q_g(r) = p_0 \exp\left[-(r/a)^2\right], \tag{1}$$

where r is the distance to the center of the source; p_0 and a are the peak source pressure and the effective source radius, respectively.

The directivity function of Gaussian source can be derived from the linear solution component by substituting (1) into the Khokhlov-Zabolotskaya-Kuznetsov (KZK) equation[5,15] under the assumption of quasilinear approximation. The KZK equation describes the entire process (diffraction, absorption and nonlinearity) of self-demodulation throughout the near-field and into the far-field, for both on-axis and off-axis of the beam, and is expressed as follows:

$$\frac{\partial^2 p}{\partial z \partial \tau} = \frac{c_0}{2}\nabla_\perp^2 p + \frac{\delta}{2c_0^3}\frac{\partial^3 p}{\partial \tau^3} + \frac{\beta}{2\rho_0 c_0^3}\frac{\partial^2 p^2}{\partial \tau^2}, \tag{2}$$

where $\nabla_\perp^2$ is the Laplacian operator that operates in the plane perpendicular to the axis of the sound beam; z is the coordinate along the beam propagation direction; p is the acoustic pressure; τ is the retarded time; δ is the diffusivity of sound; c_0 is the small-signal sound

speed; β is the coefficient of nonlinearity; and ρ_0 is the ambient density.

Thus, the far-field Gaussian directivity D_g is given by

$$D_g(\theta) = \exp\left[-\frac{1}{4}(ka)^2 \tan^2\theta\right], \tag{3}$$

where θ is the angle (in degree) with respect to the axis of the beam, and k is the wavenumber. When considering the difference frequency wave due to the radiation from a bifrequency Gaussian source, the difference frequency wave is given by the product of the directivities of the two primary frequency waves in the far-field, which is known as the PD model.[7] Let $D_1(\theta)$ and $D_2(\theta)$ denote the directivities of Gaussian sources defined by (3) at the lower primary frequency and the higher primary frequency, respectively. Thus, the directivity of the difference frequency wave is given by

$$D_{diff}(\theta) = D_1(\theta) D_2(\theta). \tag{4}$$

(b) Advanced product directivity

Our following analysis is based on {Eq. (24) in (Darvennes and Hamilton, 1990)}. Assume that the two primary Gaussian sources are concentric but steered to different angles, as shown in Fig. 1. A function of which the value is related to the relative strength of the scattered sound field, $\Gamma(\theta)$ is given by

$$\Gamma(\theta) = \frac{i\left[(z_1 + z_2)\tan\theta - (z_1 - z_2)\sin\theta_0\right]}{\sqrt{a_1^2 + a_2^2}}, \tag{5}$$

where z_1 and z_2 are Rayleigh distances for Gaussian sources at the lower primary frequency f_1 and at the higher primary frequency f_2, respectively; θ_0 is half the intersection angle of the two primary Gaussian sources.

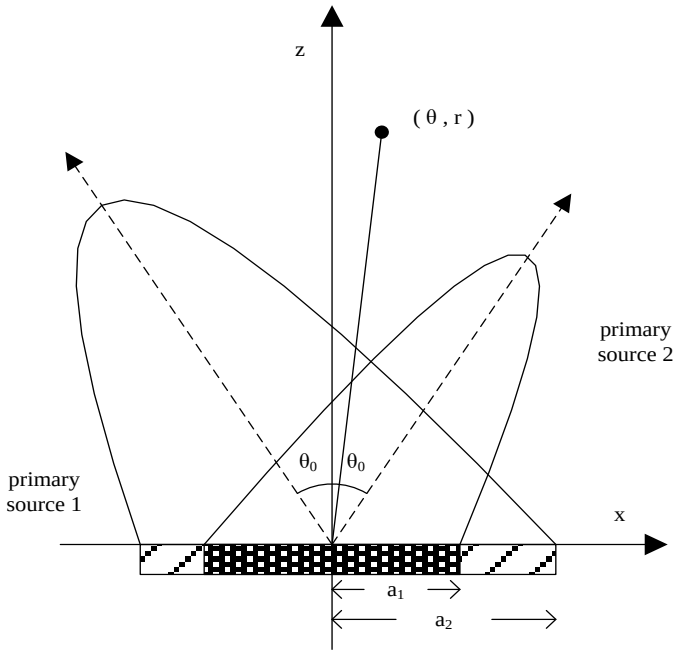

Fig.1 Symmetric source geometry for two intersecting Gaussian beams.

When $\Gamma(\theta)$ is sufficient large, i.e. $|\Gamma(\theta)| \gg 1$, an explicit expression for nonlinearly generated sound field may be obtained as

$$q_{-}(\theta,r) \approx -ip_1 p_2 k_1 k_2 k_{-} a_1^2 a_2^2 \exp\left(ik_{-} r \tan^2\theta/2\right) \times\frac{1}{8z}\left\{D_1(\theta)D_2(\theta)E_1\left[\frac{ik_1k_2\left(a_1^2+a_2^2\right)\Gamma^2(\theta)}{2k_{-}r}\right]-\frac{D_s(\theta)}{\Gamma^2(\theta)}\right\}, \quad (6)$$

where $q_{-}(\theta,r)$ is the complex pressure at the difference frequency when observation point is given by angle θ and distance r; p_1 and p_2 are the maximum on-source pressures at the lower primary frequency and the higher primary frequency, repetitively; k_1, k_2 and k_{-} are the wavenumbers of the lower primary frequency, the higher primary frequency, and the difference frequency, respectively; a_1 and a_2 are the radii of the Gaussian source of the lower primary frequency and the higher primary frequency, respectively; $D_s(\theta)$ describes the directivity of the scattered sound; and $E_1(\cdot)$ is the exponential integral.[6]

Note that the exponential integral can be extended and approximated as

$$E_1(x) = \frac{\exp(-x)}{x}\sum_{n=0}^{N-1}\frac{n!}{(-x)^n} \approx \frac{\exp(-x)}{x}, \quad \forall|x| \gg 1. \tag{7}$$

Further, if x is purely imaginary and has large magnitude, i.e. $|E_1(x)| \approx x^{-1}$. Thus, we obtain

$$\left|E_1\left[\frac{ik_1k_2\left(a_1^2+a_2^2\right)\Gamma^2(\theta)}{2k_- z}\right]\right| \approx \frac{2k_- z}{k_1k_2\left(a_1^2+a_2^2\right)\left|\Gamma^2(\theta)\right|} \tag{8}$$

Substitute (8) into (6), and by taking the absolute value on both sides of (6), we get

$$\left|q_-(\theta,z)\right| \propto \frac{p_1p_2k_-^2a_1^2a_2^2}{4\left(a_1^2+a_2^2\right)}\frac{D_1(\theta)D_2(\theta)}{\left|\Gamma^2(\theta)\right|}. \tag{9}$$

Since it is assumed that $\Gamma(\theta)$ is sufficient large, $\left|\Gamma^2(\theta)\right|$ can be treated as a constant value when θ varies in a limited range. Therefore, based on (9), we propose the advanced product directivity (APD) model for the difference frequency wave generated from the parametric loudspeaker, where the directivity of the difference frequency wave is given by

$$D_{diff}(\theta) = \frac{a_1^2a_2^2}{a_1^2+a_2^2}\,p_1D_1(\theta)\,p_2D_2(\theta). \tag{10}$$

(c) Exponential product directivity

In the Berktay's far-field solution[3], the demodulated wave along the axis of propagation is proportional to the second-time derivative of the square of the envelope of the modulated wave. If we generate two pure sine waves at the primary frequencies as the modulated wave, its frequency components are similar to a modulated wave generated by single side band modulation. Thus, the sound pressure of the difference frequency wave p_- can be computed by

$$p_- = \frac{\beta p_0^2a^2}{16\rho_0c_0^4z\delta}\frac{d^2}{d\tau^2}E^2(\tau), \tag{11}$$

where a is the source radius; p_0 is the pressure amplitude at source; and $E(\tau)$ is the

modulation envelop; the other notations have similar definitions as in the KZK equation (2).

Because of the second-time derivative in (11), the contribution to the sound pressure level generated by the parametric array varies with the square of the difference frequency ($f_{diff} = f_2 - f_1$), i.e. f_{diff}^2 . In other words, the sound pressure level at the difference frequency increases by 12 dB per octave. Equation (9) also indicates that the sound field along the propagating axis is proportional to the square of the wavenumber at the difference frequency. However, Wygant[16] fabricated their capacitive micro-machined ultrasonic transducers and tested them in both experiment and simulation (based on numerical solution to the KZK equation). Their results indicate that the sound pressure level at the difference frequency increase by 9 dB per octave, which correspond to $f_{diff}^{1.5}$. Therefore, Wygant et al. suggested that the sound pressure level of the difference frequency is proportion to f_{diff}^n , where n depends primarily on the ratio of the diffraction length (i.e. the area of the transmitter divided by the wavelength at the primary frequencies) to the absorption length (i.e. the inverse of the nominal absorption coefficient at the primary frequencies). For the Westervelt's solution[1], it was proposed that $n=2$ is a good approximation of the frequency dependence. However, for the solution obtained by Berktay and Leahy[17] and the experimental results obtained by Vos[18], $n=1$ gives better approximations of the frequency dependence in highly nonlinear distortion cases.

Based on the above methodology[16], another modification to the PD model is proposed. We refer to this model as the exponential product directivity (EPD) model, and can be written as

$$D_{diff}(\theta) = f_-^n p_1 D_1(\theta)\, p_2 D_2(\theta), \tag{12}$$

where $n \in [1,2]$ is the tuning factor[16]; and f_- is the difference frequency.

The combination of APD and EPD models, without conflicting to (8), gives the combined product directivity (CPD) model, written as

$$D_{diff}(\theta) = f_{-}^{n} \frac{a_1^2 a_2^2}{a_1^2 + a_2^2} p_1 D_1(\theta) p_2 D_2(\theta). \quad (13)$$

(d) Equivalent Gaussian source array

All the above product directivity models can only be applied to Gaussian sources. However, the ultrasonic transducer array in the parametric loudspeaker[8-14] is usually separately weighted and equally spaced, and every transducer in the linear array is assumed omnidirectional instead of Gaussian source (see Fig. 2). In one seminal paper[19] and another related survey paper[20], the authors demonstrated that it is possible to accurately simulate the sound beam of a piston source by the superposition of sufficient Gaussian beams. The coefficients are obtained by fitting the Gaussian sources to match the piston velocity distribution on the surface of the transducer using a nonlinear least squares approach. Thus, the prerequisites of the PD model can be fulfilled and the PD model can be applied to the parametric loudspeaker with a linear transducer array.[14] According to the PD model, the directivity of the difference frequency wave can be adjusted by controlling the directivity of the primary waves. A simplified structure of the beamsteerer used in the acoustic parametric array is shown in Fig. 2.

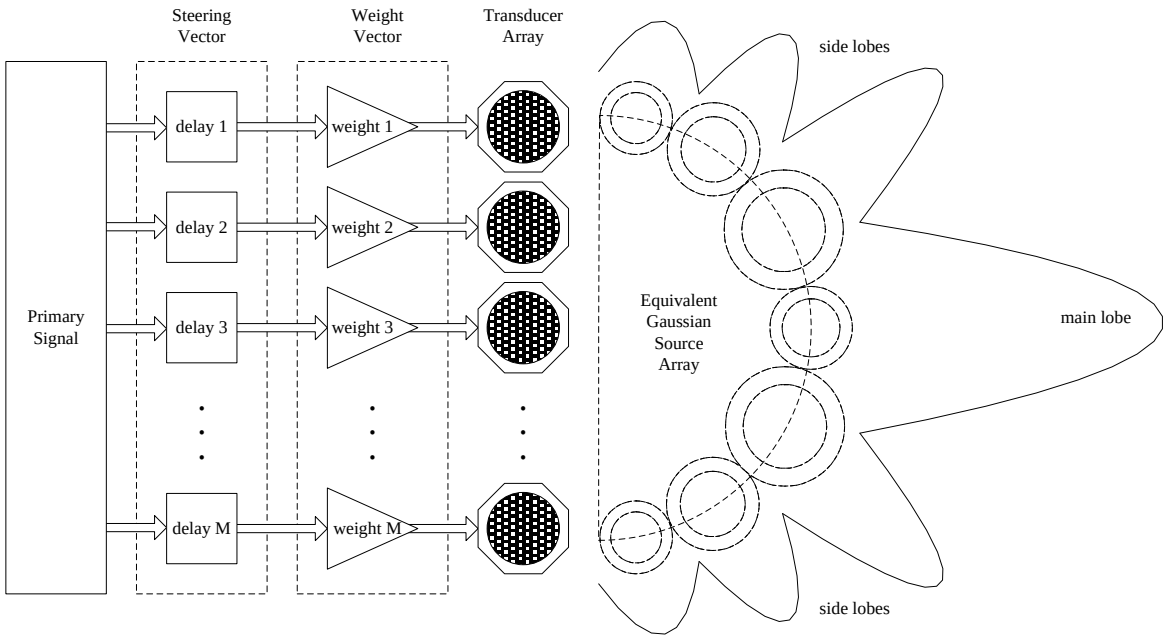

Fig. 2 Beamsteering structure for parametric loudspeaker and equivalent Gaussian source array.

Let M denote the total number of channels. Assume that the ultrasonic transducer array is steered to the same direction and shares the same group of weights for two primary frequency waves, and the difference frequency wave is also steered to the same direction. It is noted that each lobe in the beampattern of a uniform linear transducer array has a bell shape similar to the directivity of a single Gaussian source. Thus, a transformation to an equivalent Gaussian source array from a linear uniform transducer array, whose beampattern is given, can be proposed. The beampattern of the linear transducer array is denoted as $H(k,\theta)$, and the number of lobes is denoted as N. Each Gaussian source in the equivalent array corresponds to an initial pressure level B_i, an effective radius A_i and an angular offset θ_i. Therefore, the summed square of residuals over the range of angle θ is given by

$$R(k)=\left\| H(k,\theta)-\sum_{i=1}^{N} B_i \exp\left[-\frac{1}{4}(kA_i)^2 \tan^2(\theta-\theta_i)\right]\right\|_2^2. \tag{14}$$

By minimizing the value of $R(k)$, the Gaussian source array configuration that fits the beampattern of the linear transducer array best can be solved at each primary frequency.

III. MEASUREMENT AND RESULT

The beampatterns of the primary waves and the difference frequency waves were measured in an anechoic chamber with a dimension of 6 m × 3 m × 3 m. The primary waves were captured by an 1/8 inch microphone (B&K 4138). The difference frequency waves were measured using a 1/2 inch microphone (B&K 4134). The ultrasonic transducer array was configured in column-wise, as shown in Fig. 3. The ultrasonic transducer array was mounted on a motorized rotation stage, and the microphones were placed at a location 4 m away from the center of the ultrasonic transducer array. Figure 3 also shows the overall setup of the measurements. The beampatterns of the primary frequency wave, as well as the difference frequency wave were restricted to a measuring angle between -40˚ to 40˚ with a resolution of 1˚. All the channels in the ultrasonic transducer array were equally weighted, but differently delayed to achieve beamsteering. A beamsteering algorithm was implemented using a data acquisition board (NI PCI-6733) connected to a personal computer.

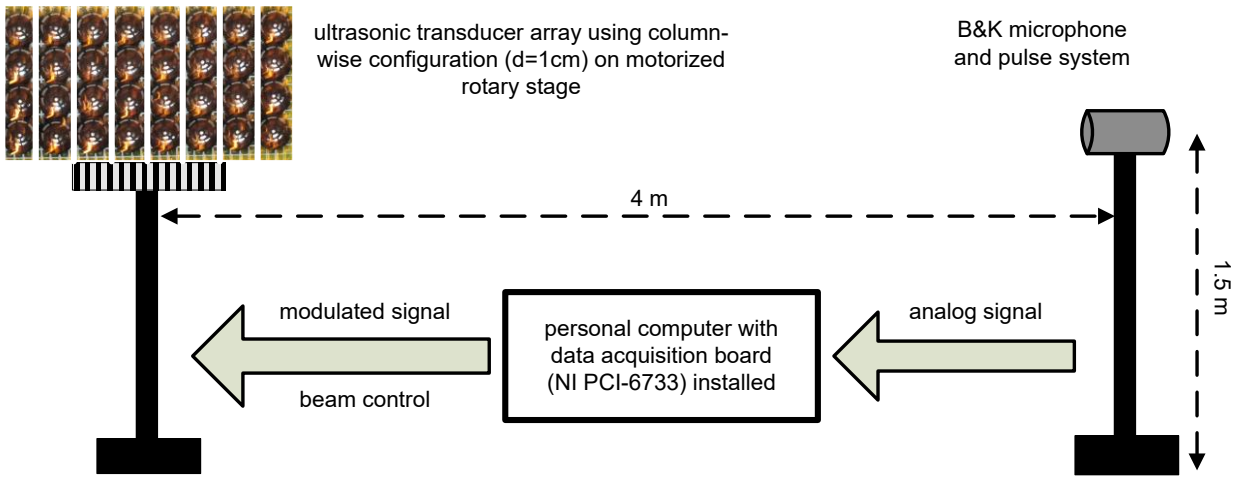

Fig. 3 The setup of the transducer array with column-wise configuration and the microphones used in the experiments.

The measured beampatterns of the primary frequencies are used to compute the configurations of the equivalent Gaussian source array. Otherwise, the system errors incurred at different stages of implementation, which include the transducer positions, transducer gain or phase response, mutual coupling, and receiver equipment effects, must be considered and compensated by array calibration approaches.[21] Both the measured beampatterns and the beampatterns of the equivalent Gaussian source array are plotted in Fig. 4 at primary frequencies of (a) 36 kHz, (b) 38 kHz, (c) 39 kHz, (d) 40 kHz, (e) 42 kHz, and (f) 44 kHz. The radii of each Gaussian source (in cm) are labeled next to its corresponding lobes as well. It is observed that the Gaussian sources corresponding to the mainlobes and the grating lobes are with relatively small radii, due to their wider beamwidths compared to other sidelobes. Significant mismatches can be observed at the troughs between two lobes where the normalized amplitudes are lower than 0.1 (i.e. -20 dB). However, the mismatches at the troughs rarely appear and are relatively slight. The least square curve fitting approach given by (14) has been proved to be adequate to derive an equivalent Gaussian source array that match the overall beampattern of the ultrasonic transducer array in the parametric loudspeaker.

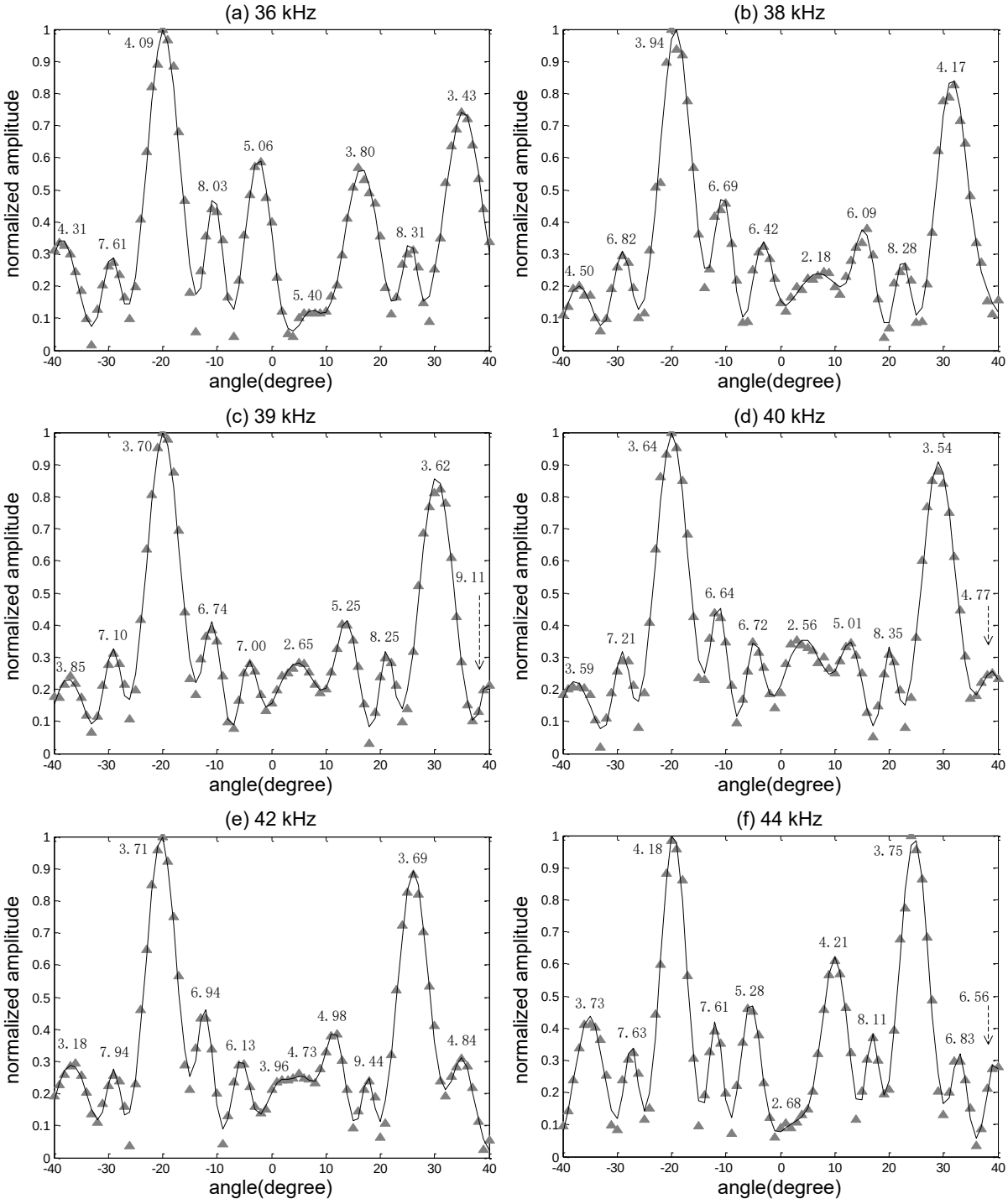

Fig. 4 The measured beampatterns (marker: ▲) and the beampatterns of equivalent Gaussian source array (solid line) at primary frequencies of (a) 36 kHz, (b) 38 kHz, (c) 39 kHz, (d) 40 kHz, (e) 42 kHz, and (f) 44 kHz. The radii of each Gaussian source (in cm) are marked next to its corresponding lobes.

From the aspect of complexity, the PD model can be applied, as long as the beampatterns of the primary frequency waves are known. In contrast, the APD model requires additional step to compute the equivalent Gaussian source array configurations from the measured beampatterns. Subsequently, the APD model is applied directly to every two Gaussian sources in the array and the resulting sound fields are summed together to obtain the beampattern of the difference frequency wave. Due to the fact that the EPD and CPD models introduce the tuning factor n in their expressions, the factor has to be determined before the EPD and CPD models can be applied. It was reported that n depends primarily on the ratio of the diffraction length (i.e. the area of the transmitter divided by the wavelength at the primary frequencies) to the absorption length (i.e. the inverse of the nominal absorption coefficient at the primary frequencies).[16] In our experiments, the primary frequencies are within a narrow band centered at 40 kHz. Therefore, the wavelength and the absorption coefficient can be approximately constant. Furthermore, we consider the intersection of two Gaussian sources rather than a single transmitter in the reference. The area of the transmitter is therefore approximated by the product of the radii of the two Gaussian sources. Thus, the tuning factor is proposed in the form of

$$n = \varepsilon a_1 a_2 + 1, \tag{15}$$

where ε is computed from the measured beampatterns of the difference frequency wave at 8 kHz. For the EPD model, $\varepsilon = 39.4$. For the CPD model, $\varepsilon = 7.8$. Once the tuning factor is determined, the EPD and CPD models can be applied to the measured beampatterns of the primary frequency waves to predict the beampatterns of the difference frequency waves at 1 kHz and 4 kHz.

The beampatterns predicted by the three proposed models (APD, EPD, and CPD) are compared with the measured beampattern (MP) as well as the beampatterns based on the PD

model. Figure 5 shows the difference frequency at (a) 1 kHz, (b) 4 kHz, and (c) 8 kHz. Table I shows the normalized amplitudes of selected sidelobes (labeled in Fig. 5 as “S1”, “S2”, “S3”, and “S4”) and the grating lobe (labeled as “G”) in the measured beampatterns (MP) versus the numerical solutions to different product directivity models. Note that when the difference frequency is 8 kHz, the numerical solutions to the EPD and CPD models are not available for comparison, as the tuning factors for both the EPD and CPD models are computed based on the measured beampatterns at 8 kHz.

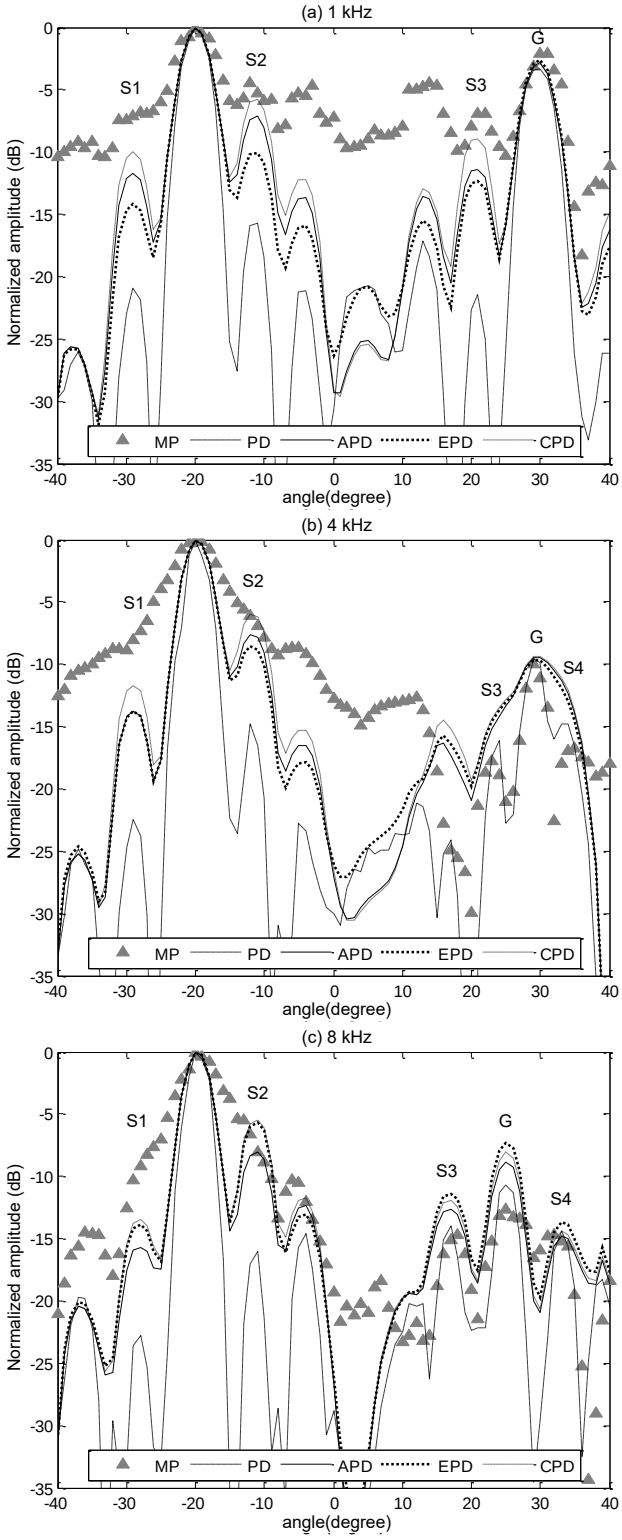

Fig. 5 The measured beampatterns (MP), the beampatterns computed by product directivity (PD) model , advanced product directivity (APD) model, exponential product directivity (EPD) model, and combined product directivity (CPD) model at the difference frequencies of (a) 1 kHz, (b) 4 kHz, (c) 8 kHz.

Table I The normalized amplitudes of selected sidelobes and the grating lobe in the beampatterns of measurement, APD model, EPD model, CPD model and PD model at the difference frequencies of 1 kHz, 4 kHz, and 8 kHz.

Diff. Freq.	1 kHz				4 kHz					8 kHz				
Lobe Label	S1	S2	S3	G	S1	S2	S3	G	S4	S1	S2	S3	G	S4
Loc (degree)	-29	-12	21	30	-29	-12	23	29	35	-28	-11	-17	25	33
MP (dB)	-7.087	-4.46	-6.95	-2.087	-8.073	-6.127	-17.77	-9.983	-16.78	-9.17	-8.07	-15.06	-12.66	-15.24
APD (dB)	-11.69	-7.387	-11.37	-2.864	-13.77	-7.595	-15.19	-9.466	-13.88	-15.67	-8.036	-12.66	-8.822	-14.78
EPD (dB)	-14.19	-10.17	-12.36	-2.591	-13.79	-8.536	-14.58	-9.652	-14.51	n.a.	n.a.	n.a.	n.a.	n.a.
CPD (dB)	-10	-6.012	-8.934	-2.894	-11.67	-5.957	-14.37	-9.409	-13.64	n.a.	n.a.	n.a.	n.a.	n.a.
PD (dB)	-20.91	-15.94	-21.42	-3.317	-22.45	-14.81	-17.45	-9.577	-16.57	-22.74	-16.06	-13.98	-10.74	-14.36

In Fig. 5(a), the CPD model gives the best prediction of the three sidelobes adjacent to the mainlobe and the grating lobe at the difference frequency of 1 kHz. The APD and EPD models give comparatively good prediction as well. A 10 dB improvement in predicting the sidelobes is observed using the CPD model when compared to the PD model. Among the 3 models, the EPD model has the best performance in predicting the grating lobe. All proposed models have better grating lobe performance compared to the PD model, though the improvements are moderate.

In Fig. 5(b), the CPD model gives the best prediction of the two sidelobes adjacent to the mainlobe at the difference frequency of 4 kHz. The improvement between the CPD model and the PD model achieves 10.78 dB and 8.85 dB for the sidelobes labeled as “S1” and “S2”, respectively. The PD model gives the best prediction of the sidelobe adjacent to the grating lobe, and the EPD model gives the best prediction of the grating lobe. However, all product directivity models perform similarly in term of predictions of the grating lobe and sidelobes adjacent to the grating lobe.

Figure 5(c) shows the performance at the difference frequency of 8 kHz. As mentioned above, the results of the EPD and CPD models are not taken into comparison. The APD model outperforms the PD model for the three sidelobes labeled as “S1”, “S2”, and “S4”, but does not predict the grating lobe and the sidelobe labeled as “S3” well.

It is concluded based on the comparison results that all the proposed models outperform the PD model in terms of prediction of sidelobes adjacent to the mainlobe. However, when the grating lobe is eliminated, the PD model can be used to predict the grating lobe and the sidelobes adjacent to the grating lobe without lose of accuracy, although the prediction of the eliminated grating lobe is not of importance to the beampattern design of the parametric loudspeaker. In terms of overall performance, the APD model is recommended when the grating lobe is not significantly eliminated. Another advantage of the APD model is its simplicity that it can be readily applied once the beampatterns of the primary frequency waves are known. Both the EPD and CPD models require additional measurement results to determine the tuning factor. The CPD model is found to give more accurate predictions to the overall beampatterns of the difference frequency waves, in comparison to the EPD model that can only predict the amplitude of the grating lobe accurately.

IV. CONCLUSION

In this paper, we proposed three modified product directivity models, namely (i) the advanced product directivity model, (ii) the exponential product directivity model, and (iii) the combined product directivity model. All the proposed product directivity models are based on the transformation of linear transducer array to an equivalent Gaussian source array, and taking the radii of the Gaussian sources into account to obtain better predictions of beampatterns of the difference frequency waves. Based on the comparison between measurement results and numerical solutions, all the proposed models outperform the PD model in terms of prediction of sidelobes adjacent to the mainlobe. The advantage of the APD model is its simplicity that it can be readily applied once the beampatterns of the primary frequency waves are measured or computed based on calibration methods. When the grating lobe is eliminated, the PD model can

be used to predict the grating lobe and the sidelobes adjacent to the grating lobe without lose of accuracy. Though in the case of grating lobe elimination, the prediction of the grating lobe is not important to the beampattern design of the parametric loudspeaker, the PD model remains a good and simple model to determine the level of grating lobe elimination. Judged by overall performance, the APD model is recommended when the grating lobe is not significantly eliminated. When additional measurements can be conducted to determine the tuning factor, the CPD model is found to give more accurate predictions to the overall beampatterns of the difference frequency waves, compared to the EPD model that can only predict the amplitude of the grating lobe accurately.

ACKNOWLEDGE

This work is partially supported by the Singapore National Research Foundation Interactive Digital Media R&D Program, under research grant NRF2007IDM-IDM002-086; and the Singapore Ministry of Education Academic Research Fund Tie-2, under research grant MOE2010-T2-2-040.

REFERENCES

[1]P. J. Westervelt, “Parametric acoustic array,” J. Acoust. Soc. Am., **35**, 535-537(1963).

[2]M. B. Bennett and D. T. Blackstock, “Parametric array in air,” J. Acoust. Soc. Am, **57**, 562-568 (1975).

[3]H. O. Berktay, “Possible exploitation of non-linear acoustics in underwater transmitting applications,” J. Sound Vib., **2**, 435-461 (1965).

[4]W. S. Gan, E. L. Tan and S. M. Kuo, “Audio Projection: Directional sound and its application in immersive communication,” IEEE Signal Processing Mag., **28**, 53-57 (2011).

[5]E. A. Zabolotskaya and R. V. Khokhlov, “Quasi-plane waves in the nonlinear acoustics of confined beams,” Sov. Phys. Acoust., **15**, 35-40 (1969).

[6]C. M. Darvennes and M. F. Hamilton, “Scattering of sound by sound from two Gaussian beams,” J. Acoust. Soc. Am., **87**, 1955-1964 (1990).

[7]M. F. Hamilton, “Sound Beams,” in *Nonlinear Acoustics*, edited by M. F. Hamilton and D. T. Blackstock (Academic Press, San Diego, 1998), Chap. 8, pp. 233-261.

[8]K. S. Tan, W. S. Gan, J. Yang, and M. H. Er, “Constant beamwidth beamformer for difference frequency in parametric array”, Proc. Int. Conf. Multimedia. Expo, **2**, 593-596 (2003).

[9]D. Olszewski, F. Prasetyo, and K. Linhard, “Steerable highly directional audio beam loudspeaker”, Proc. Interspeech, 137-140 (2005).

[10]W. S. Gan, J. Yang, K. S. Tan, M. H. Er, “A digital beamsteerer for difference frequency in parametric array,” IEEE Trans. on Audio, Speech and Language Processing, **14**, 1018-1025 (2006).

[11]C. H. Lee, J. B, D. G. Paeng, J. Lee and S. Kim, “Digital beamsteering system using acoustic transducer array,” J. Acoust. Soc. Am., **129**, 2675-2675 (2011).

[12]N. Tanaka and M. Tanaka, “Active noise control using a steerable parametric array loudspeaker,” J. Acoust. Soc. Am., **127**, 3526-3537 (2010).

[13]N. Tanaka and M. Tanaka, “Mathematically trivial control of sound using a parametric beam focusing source,” J. Acoust. Soc. Am., **129**, 165-172 (2011).

[14]C. Shi and W. S. Gan, “Grating lobe elimination in steerable parametric loudspeaker,” IEEE Trans. Ultrason. Ferroelectr. Freq. Control, **58**, 437-450 (2011).

[15]V. P. Kuznetsov, “Equations of nonlinear acoustics,” Sov. Phys. Acoust., **16**, 467-470 (1971).

[16]I. O. Wygant, M.Kupnik, J. C. Windsor, W. M. Wright, M. S. Wochner, G. G. Yaralioglu, M. F. Hamilton, and B. T. Khuri-Yakub, “50 kHz capacitive micromachined ultrasonic transducers for generation of highly directional sound with parametric arrays,” IEEE Trans. Ultrason. Ferroelectr. Freq. Control, **56**, 193-203 (2009).

[17]H. O. Berktay and D. J. Leahy, “Farfield performance of parametric transmitters,” J. Acoust. Soc. Am., **55**, 539–546 (1974).

[18]H. J. Vos, D. E. Goertz, A. F. W. van der Steen and N. de Jong, “Parametric array technique for microbubbleexcitation,” IEEE Trans. Ultrason. Ferroelectr. Freq. Control, **58**, 924-934 (2011).

[19]J. J. Wen and M. A. Breazeale, “A diffraction beam field expressed as the superposition of Gaussian beams,” J. Acoust. Soc. Am., **83**, 1752–1756 (1988).

[20]H. J. Kim, L. W. Schmerr and A.Sedov, “Generation of the basis sets for multi-Gaussian ultrasonic beam models—An overview,” J. Acoust. Soc. Am., **119**, 1971-1978 (2006).

[21]D. H. Johnson and D. E. Dudgeon, “Beamforming,” in *Array Signal Processing: Concepts and Techniques*, edited by D. H. Johnson and D. E. Dudgeon (Prentice Hall, New Jersey, 1993), Chap.4, pp. 111-198.

Table I The normalized amplitudes of selected sidelobes and the grating lobe in the beampatterns of measurement, APD model, EPD model, CPD model and PD model at the difference frequencies of 1 kHz, 4 kHz, and 8 kHz.

Diff. Freq.	1 kHz				4 kHz					8 kHz				
Lobe Label	S1	S2	S3	G	S1	S2	S3	G	S4	S1	S2	S3	G	S4
Loc (degree)	-29	-12	21	30	-29	-12	23	29	35	-28	-11	-17	25	33
MP (dB)	-7.087	-4.46	-6.95	-2.087	-8.073	-6.127	-17.77	-9.983	-16.78	-9.17	-8.07	-15.06	-12.66	-15.24
APD (dB)	-11.69	-7.387	-11.37	-2.864	-13.77	-7.595	-15.19	-9.466	-13.88	-15.67	-8.036	-12.66	-8.822	-14.78
EPD (dB)	-14.19	-10.17	-12.36	-2.591	-13.79	-8.536	-14.58	-9.652	-14.51	n.a.	n.a.	n.a.	n.a.	n.a.
CPD (dB)	-10	-6.012	-8.934	-2.894	-11.67	-5.957	-14.37	-9.409	-13.64	n.a.	n.a.	n.a.	n.a.	n.a.
PD (dB)	-20.91	-15.94	-21.42	-3.317	-22.45	-14.81	-17.45	-9.577	-16.57	-22.74	-16.06	-13.98	-10.74	-14.36

LIST OF FIGURES